Physica C 204 (1992) 171–178
North-Holland

PHYSICA C

Magnetic ordering of the Cu spins in $PrBa_2Cu_3O_{6+x}$

N. Rosov and J.W. Lynn
Reactor Radiation Division, National Institute of Standards and Technology, Gaithersburg, MD 20899, USA, and Center for Superconductivity Research, Department of Physics, University of Maryland, College Park, MD 20742, USA

G. Cao, J.W. O'Reilly, P. Pernambuco-Wise and J.E. Crow
National High Magnetic Field Laboratory, Florida State University, Tallahassee, FL 32306, USA

Received 8 October 1992

Neutron diffraction has been employed to investigate the magnetic ordering of the Cu spins in a single crystal of $PrBa_2Cu_3O_{6+x}$. At small x we have observed a Néel temperature T_N of 370 K, where both the chain and plane Cu spins order simultaneously. For $x \sim 0.6$, the Cu planes still order at $T_N \sim 370$ K; however, the ordering temperature of the chain spins has decreased to ~ 160 K. The observed intensities of the magnetic reflections cannot be explained by keeping the chain layer Cu spin direction in the *ab* plane; rather, the chain moments must have a component along the *c* direction. We dicuss these results in light of recent optical reflectivity measurements on $PrBa_2Cu_3O_{6+x}$ by Takenaka et al. [Phys. Rev. B 46 (1992) 5833].

1. Introduction

The layered perovskite compounds $\mathscr{R}Ba_2Cu_3O_{6+x}$ ($\mathscr{R}1236+x$) display a wealth of interesting properties [1]: high-temperature superconductivity, metal–insulator phase transition, structural phase transitions, and two-dimensional magnetic order, to name but a few. Many of these properties are affected by varying the component atoms at particular sites in the $\mathscr{R}1236+x$ compounds. However, the rare earth site $\mathscr{R}$ in $\mathscr{R}1236+x$ can be replaced by many of the rare-earth elements with little effect on the superconductivity. An exception to this occurs for Pr, where even fully oxygenated Pr1237 is not superconducting [2]. Measurements of the effect of Pr on the properties of $\mathscr{R}1237$ [3] are important in order to gain insight into the mechanism of superconductivity in the layered perovskites.

The lack of superconductivity in Pr1237 is thought to be related to the hybridization of the Pr wavefunction at the Fermi level [3]. The antiferromagnetic ordering of Pr in Pr1237 at 17 K [4] – a temperature at least two orders-of-magnitude higher than expected by a purely dipolar interaction, such as is seen in other $\mathscr{R}1237$ compounds [5] – indicates that the Pr ions are strongly coupled through the CuO_2 planes. Inelastic neutron scattering results [6,7] show quite broad crystal field excitations, which have been successfully interpreted in light of the crystal-field splitting of exchange-coupled Pr [7].

There are three copper layers in the $\mathscr{R}1236+x$ structure. Two of these layers, the so-called "plane" layers, consist of Cu(2) sites, which are in a pyramidal coordination, bonded by O^2-ions along both the *a*- and *b*-axes. The third layer, the "chain" layer, is composed of Cu(1) sites, which are in a planar coordination, bonded by O^2-along the *b*-axis. At $x \approx 0$, there are no oxygen ions directly between the Cu(1), but as the oxygen content is increased to $x=1$, Cu(1)–O^{2-}–Cu(1) chains are formed. The $\mathscr{R}$ layers are sandwiched between the Cu(2) layers, and the Cu(1) layer is sandwiched between the Ba layers: the sequence along the *c*-axis is Cu(2)–Ba–Cu(1)–Ba–Cu(2)–$\mathscr{R}$–Cu(2).

For all the rare earths that form the 123 crystal structure, with the exception of Pr, the Cu spins only order for $x \lesssim 0.5$, where the materials are non-conducting. At $x=0$ the Cu(2) spins order at $T_{Np} \approx 525$ K in a simple antiferromagnetic structure, with nearest neighbors antiparallel along all three axes, as

0921-4534/92/$05.00 © 1992 Elsevier Science Publishers B.V. All rights reserved.

shown in fig. 1(a). As there is one Cu(2) per unit cell along the a and b directions, while there are two Cu(2) layers per unit cell along the c direction, the antiferromagnetic unit cell is double the chemical unit cell along a and b only. As a result, this so-called "plane" ordering is characterized by magnetic Bragg reflections $(\frac{mn}{22}, l)$, where l is a whole integer. These are referred to as "whole-integral" reflections. Below the Néel temperature T_{Np}, the intensities of these whole-integral reflections, which are directly related to the sublattice magnetization, increase with decreasing temperature as the average ordered moment increases.

At a lower temperature ($T_{Nc} \approx 80$ K for $x \approx 0.1$), the "chain" Cu(1) spins also been observed to order in some samples [1,8,9]. Since the basic interaction between the layers is antiferromagnetic and the neighboring Cu(2) planes are already antiferromagnetically aligned, the competition between the two antiferromagnetic stacking arrangements causes Cu(1) spins to order in a direction orthogonal to the Cu(2) spins, producing a non-collinear spin structure, as shown in fig. 1(b). This non-collinear spin structure is evidenced by the observation of a combination of whole-integral "plane-ordering" reflections and a new set of "half-integral" $(\frac{mnl}{222})$ reflections. The new reflections indicate that we have a new magnetic unit cell that is now doubled along the c-axis. Below the second ordering temperature T_{Nc}, the half-integral reflections increase in intensity with decreasing T, while the whole-integral reflections decrease in intensity. As T approaches 0 K, the spin structure tends to a collinear ground state, where the whole-integral reflections have vanishing intensity and only the half-integral reflections survive.

As x increases from 0.1, the plane and chain ordering temperatures both decrease, indicating that the Cu magnetism is related sensitively to the electronic structure of both the chain and plane layers. In fact, the chains have a very large magnetic susceptibility: the chain ordering temperature is dramatically increased (to the plane ordering temperature) by doping Co into the Cu(1) site [10] or doping Nd into the Ba site [11]. The presence of plane order itself appears to increase the chain ordering temperature: $T_{Nc} \approx 80$ K for Nd1236.1 [8], whereas $T_{Nc} = 4.3$ K for Sr_2CuO_3, an infinite Cu chain compound with no Cu planes [12]. We have studied the Cu magnetism in Pr1236+x to compare with the behavior of the other $\mathscr{R}$1236+x compounds and to

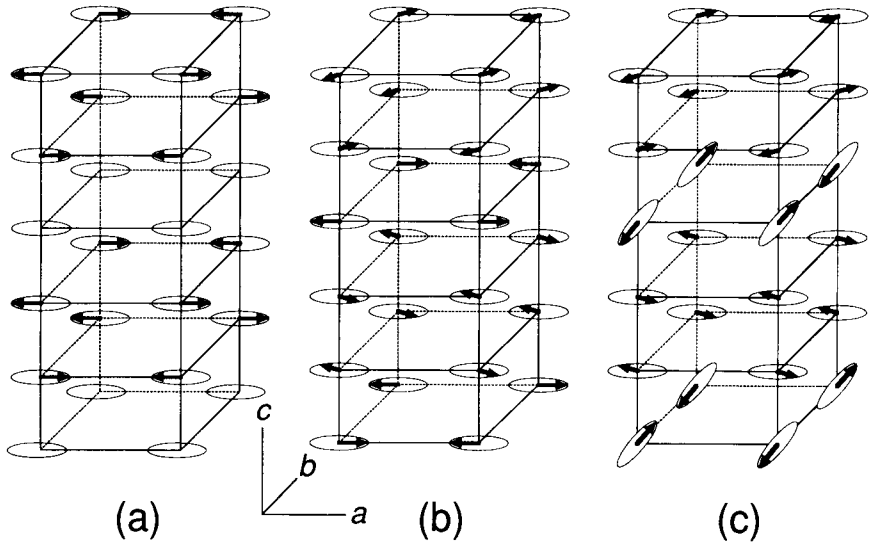

Fig. 1. Moment directions for the magnetic structures of (a) the plane-only ordered state of Pr123 and Nd123, (b) the plane and chain ordered state of Nd123, and (c) the plane and chain ordered state of Pr123, where the Cu chain moments have a significant component along the c-axis. The arrows are all unit vectors and the apparent length changes are due only to foreshortening.

further elucidate the effect of Pr on these layered perovskites.

2. Sample characterization, oxygen concentration, and magnetic ordering of Cu chains and planes

Our sample of $PrBa_2Cu_3O_{6+x}$ was a single crystal with dimensions $4\times2.5\times0.5$ mm^3 grown from a $BaCO_3$/CuO self flux by spontaneous crystallization [13]. We measured this sample at four oxygen concentrations, which we label as x_1, x_2, x_3, and x_4: the as grown crystal, Pr1236+x_1; Pr1236+x_2, which was annealed in one atmosphere of O_2 at 450°C for fourteen days; Pr1236+x_3, which was annealed in hyperbaric (20 MPa) O_2 at 500°C for 14 days; and Pr1236+x_4, which was annealed in vacuum at 450°C for 14 days.

The neutron diffraction measurements were performed at the National Institute of Standards and Technology Research Reactor on the BT-2, BT-4, BT-6, and BT-9 spectrometers. These are all standard triple-axis spectrometers, which were operated in two-axis mode for these measurements. A pyrolytic graphite (PG) monochromator was employed in each case, and a wavelength of $\lambda=2.35$ Å was chosen so that a PG filter could be used to suppress higher-order wavelength contaminations. Typical collimations for the magnetic measurements were 60′–40′–Sample–40′. The sample was aligned so that (*hhl*) reflections were in the scattering plane. Integrated intensities of the reflections were obtained by rotating the sample at constant $2\theta_B$ through the Bragg peak.

The magnetic scattering intensity is given by [14]

$$I_m = CL\left\langle \left| \sum_{j=1}^{n} p_j(\hat{\boldsymbol{\tau}}(\hat{\boldsymbol{\tau}}\cdot\hat{\boldsymbol{M}}_j)\, e^{i\boldsymbol{\tau}\cdot\boldsymbol{r}_j} e^{-W_j} \right|^2 \right\rangle_D , \qquad (1)$$

where C is an instrumental constant, L is the Lorentz factor (which in the case of sample rocking scans is $[\sin(2\theta_B)]^{-1}$), W_j is the Debye–Waller factor, $\boldsymbol{\tau}$ is the reciprocal lattice vector, and $\hat{\boldsymbol{M}}_j$ is a unit vector in the direction of the spin at site j, located at position $\boldsymbol{r}_j$. The magnetic scattering amplitude for the jth magnetic ion is given by

$$p_j = \frac{\gamma e^2}{2mc^2} \langle \mu_j \rangle f_j(\boldsymbol{\tau}) , \qquad (2)$$

where the numerical coefficient is -0.27×10^{-12} cm, $\langle \mu_j \rangle$ is the thermal average of the moment at site j, and $f_j(\boldsymbol{\tau})$ is the magnetic form factor, which is the Fourier transform of the atomic magnetization density due to the jth atom. The summation in eq. (1) over all n atoms in the unit cell is the magnetic structure factor, which we note in the present case is a vector quantity as we must consider the general case of non-collinear magnetic structures.

The single crystal X-ray diffraction measurements were made at the University of Maryland with a rotating anode diffractometer. We used $\bar{\lambda}=1.545178$ Å Cu Kα radation reflected from a vertically focusing pyrolytic graphite (002) monochromator. For these measurements, the crystal was aligned so that (*h*0*l*) reflections were in the scattering plane.

2.1. Pr1236+x_1

The single crystal was of high quality, and we typically observed rocking curves that were resolution limited, both for the structure peaks observed with neutrons or X-rays as well as for the magnetic Bragg peaks. Our crystal growth technique produces as-grown crystals that are quite oxygen-deficient, and we estimate $x_1 \sim 0.2$ based on susceptibility and magnetization data. Our neutron scattering measurements showed that the as-grown crystal ordered antiferromagnetically at $T_N \approx 370$ K, and over the entire temperature range 20 K $\leq T \leq$ 340 K, we observed only half-integral peaks. The absence of whole-integral peaks demonstrates that at this oxygen concentration both the Cu plane spins and the Cu chains spins order together at the same temperature.

The temperature dependence of the intensity of the strongest magnetic Bragg peak, the $(\frac{1}{2}\frac{1}{2}\frac{3}{2})$ reflection, is shown in fig. 2. The data at high T are limited to 340 K by the cryogenic equipment that was available for these measurements. The solid curve is a fit to an $S=\frac{1}{2}$ mean field model, which we used as a guide to the eye, as well as to estimate the Néel temperature. The mean-field fit yields an ordering temperature of 390 K. However, this fitting procedure is known to give an overestimate of the actual Néel temperature. We discuss this point in more detail when we present our data for the x_4 sample, for which we obtained data over the entire temperature range

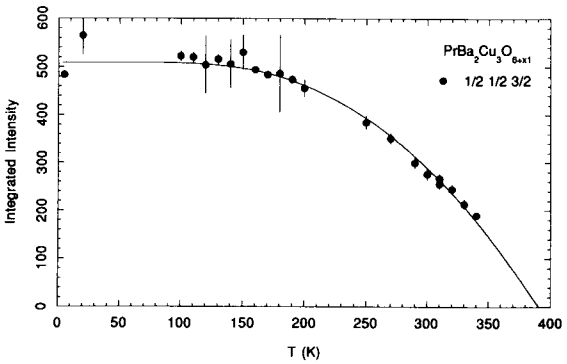

Fig. 2. Temperature dependence of combined plane and chain ordering for Pr1236+x_1, as given by the intensity of the $(\frac{1}{2}\frac{1}{2}\frac{3}{2})$ reflection. The solid curve is a fit of the data to the square of a spin-$\frac{1}{2}$ Brillouin function.

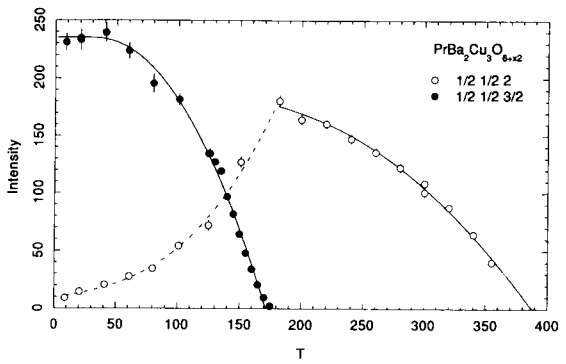

Fig. 3. Temperature dependence of plane and chain ordering for Pr1236+x_2, as given by the intensity of the $(\frac{1}{2}\frac{1}{2}2)$ and $(\frac{1}{2}\frac{1}{2}\frac{3}{2})$ reflections. The Cu(2) moments order at $T_{Np} \approx 370$ K, whereas the Cu chain moments also become ordered below $T_{Nc} \approx 160$ K. The decrease in the $(\frac{1}{2}\frac{1}{2}2)$ intensity and the concomitant increase in the $(\frac{1}{2}\frac{1}{2}\frac{3}{2})$ intensity are due to the conversion from the spin structure of fig. 1(a), above T_{Nc}, to the spin structure of fig. 1(c), below T_{Nc}. The solid curves are a fit of the data to the square of a spin-$\frac{1}{2}$ Brillouin function; see text for a discussion of the estimate of T_{Np}. The dashed curve is a guide to the eye.

of interest. Taking this overestimate into account, we estimate $T_N = T_{Nc} = T_{Np} \approx 370$ K. Such a high chain-ordering temperature has only been observed in substitutional systems in which the electronic structure is affected, such as introducing Co on the chain site [10], or Nd on the Ba site [11], and is further evidence that the Pr is significantly affecting the electronic structure of the system. This is in sharp contrast to the observed behavior of the other $\mathscr{R}1236+x$ compounds, where the maximal observed $T_{Nc} \approx 80$ K.

2.2. *Pr1236+x_2*

The single crystal was annealed at 450°C in one atmosphere of O_2 for 14 days, and then the magnetic scattering was remeasured. In the temperature range 355 K $\geq T \geq$ 170 K, we observed only whole-integral peaks, and thus in this temperature regime, only the Cu(2) spins are ordered. The temperature dependence of the strongest whole-integral peak, the $(\frac{1}{2}\frac{1}{2}2)$ reflection, is shown in fig. 3. Above 170 K, the data again follow an $S=\frac{1}{2}$ mean field model fit, and we obtained an ordering temperature from the fit of 390 K, just as for the as-grown sample. Hence, we estimate $T_{Np} \approx 370$ K. The change in oxygen concentration (see below) therefore has not affected T_{Np}, in sharp contrast to the behavior observed in all the other $\mathscr{R}1236+x$ systems. In fact, we find that T_{Np} is independent of the oxygen concentration to within our experimental accuracy over the range of oxygen concentration explored (up to $x \simeq 0.65$).

Below $T \approx 170$ K, fig. 3 shows that the whole-integral peak intensities start decreasing, while new half-integral peaks are observed that increase with decreasing temperature. At low temperatures the half-integral peaks saturate in intensity, while the whole-integral peaks become very small in intensity. This is identical to the behavior observed in the Nd1236+x [8] system, and indicates that the chain spins are becoming ordered below $T_{Nc} \approx 170$ K. We will discuss the details of the spin structures and the values of the ordered moments below.

It is clear that increasing the oxygen content is strongly detrimental to the ordering of the chain spins, as T_{Nc} has decreased from 370 K to 170 K. Nevertheless, the powder data taken [4] to observe the Pr ordering at low temperature (17 K) did not indicate any chain ordering in the fully oxygenated material. In addition, μSR data [15,16] at $x=1$ show that just a single site orders, at ~275 K, whereas at small x, two sites are observed, with T_N above room temperature. Thus it is likely that the present oxygen anneal on the single crystal has not resulted in full oxygen stoichiometry. One straightforward way of determining the absolute oxygen concentration is via neutron profile refinenment on a powder, but of

course this technique is not applicable to single crystals, and thermogravimetric measurements only provide relative oxygen concentrations. In an effort to determine the oxygen concentrations in the single crystal, we used X-ray techniques to make a precise determination of the room temperature lattice constants, and then related these to the oxygen content via the experimentally-determined phase diagram of López-Morales et al. [17]. Unfortunately, the lattice constants of Pr1236+x have very little dependence on the oxygen concentration except in the vicinity of the orthorhombic–tetragonal transition, so this technique only enables one to determine whether the oxygen concentration is above, below, or near that of the orthorhombic–tetragonal transition ($x \simeq 0.65$).

We measured the Bragg angles, $2\theta_B$, of the ($h00$) ($1 \le h \le 4$) and ($00l$) ($1 \le l \le 14$) reflections with θ–2θ scans. We then determined the lattice parameters by a least-squares fit to, e.g., in the case of the c-axis,

$$d = \frac{l}{c} = \frac{2}{\lambda} \sin(\theta_B + \varphi_0) \,. \qquad (3)$$

Figure 4 shows the data for the x_2 concentration. The lattice constants of Pr1236+x_2 are found to be $a = 3.896(1)$ Å, $b = 3.921(1)$ Å, and $c = 11.729(2)$ Å, with a slight amount of twinning observed. We also examined the (200) reflection using $\lambda = 2.35$ Å neutrons and tight collimation (10′–10′–10′–20′) with a PG(002) analyzer crystal, and observed *no* twinning, leading us to believe that the vast majority of the sample is on the oxgygen-deficient side of the orthorhombic–tetragonal transition. The combination of the X-ray and neutron observations suggests that the sample is at the orthorhombic–tetragonal transition, i.e., $x_2 \simeq 0.65$ [17].

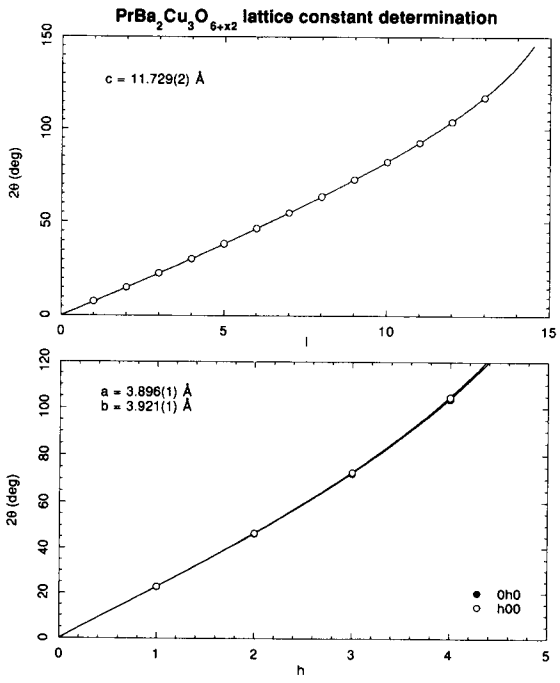

Fig. 4. Observed X-ray Bragg angles as a function of index for ($00l$) (top) and ($h00$) (bottom) reflections. The observation of an orthorhombic splitting with the X-ray measurements and the lack of the same for the neutron measurements, as well as the derived lattice parameters from the X-ray measurements, imply that $x_2 \sim 0.65$. The solid curves are the results of least squares fits to eq. (3).

2.3. *Pr1236+x_3*

A hyperbaric (20 MPa) O_2 anneal of the sample was performed with $T = 500$°C for 14 days at AT&T Bell Laboratories in an attempt to fully oxygenate the sample. The mass of the crystal changed from 11.012 mg before the hyperbaric anneal to 11.016 mg after. This weight change implies that the difference $x_3 - x_2 \approx 0.016$, a very small change. Neutron magnetic diffraction data were then retaken. In the range $350\ \text{K} \ge T \ge 240\ \text{K}$, only the whole-integral peaks are observed, as shown in fig. 5. Fitting the data to an $S = \frac{1}{2}$ mean field model yields an ordering temperature of 425 K, and thus we estimate an increased $T_{Np} \approx 405$ K.Between 180 K and 240 K a slight amount of helf-integral intensity appears, while the whole-integral intensity goes through a slight dip as shown. Below 180 K, the half-integral intensity strongly increases as the whole-integral intensity decreases, as seen previously for the x_2 sample, but with a slightly higher chain-ordering temperature. We also measured, via X-rays as described above, the room temperature lattice parameters, and found $a = 3.882(4)$ Å, $b = 3.9142(4)$ Å, and $c = 11.720(5)$ Å, with a significant amount of twinning. These parameters are not consistent with the phase diagram of López-Morales et al. [17], and we suspect that the surface region of the sample may be affected by the hyperbaric O_2 treatment. It appears as if the sample

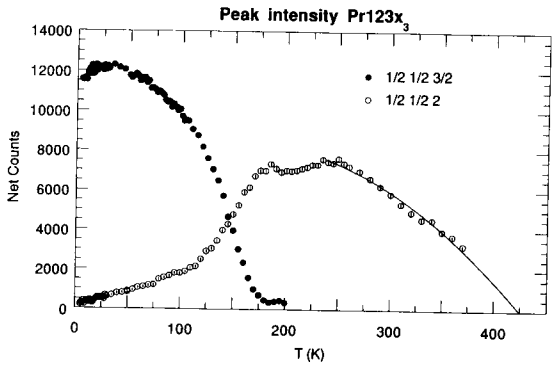

Fig. 5. Temperature dependence of plane and chain ordering for Pr1236+x_3, as given by the intensity of the $(\frac{1}{2}\frac{1}{2}2)$ and $(\frac{1}{2}\frac{1}{2}\frac{3}{2})$ reflections. The Cu(2) moments order at $T_{Np} \approx 405$ K, whereas both the plane and chain Cu moments are ordered below $T_{Nc} \approx 180$ K. The behavior of the intensity in the region between 180 K and 240 K suggests that the sample has become multi-phase as a result of the hyperbaric oxygen treatment. The solid curve is a fit of the data to the square of a spin-$\frac{1}{2}$ Brillouin function; the difference between the T_{Np} and the Brillouin fitted value is discussed in the text.

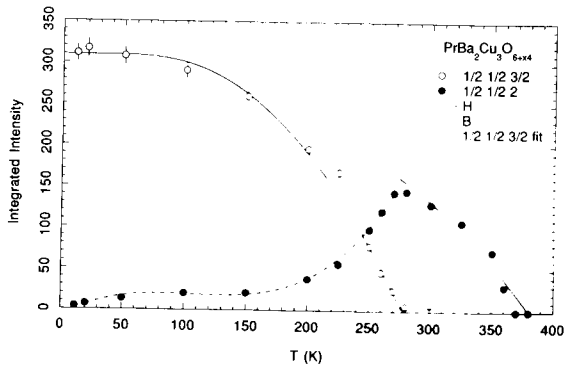

Fig. 6. Temperature dependence of plane and chain ordering for Pr1236+x_4, as given by the intensity of the $(\frac{1}{2}\frac{1}{2}2)$ and $(\frac{1}{2}\frac{1}{2}\frac{3}{2})$ reflections. The Cu(2) moments order at $T_{Np} \approx 370$ K, whereas both the plane and chain Cu moments are ordered below $T_{Nc} \approx 280$ K. The solid curve is a fit of the data to the square of a Brillouin function. The dashed curve is a guide to the eye. Note that the Brillouin fitted value overestimates T_{Np} as discussed in the text.

has become multiphase, with parts of the sample ordering at different temperatures.

2.4. Pr1236+x_4

The final anneal of the sample was in vacuum at 450°C for 14 days, in order to remove oxygen. Unfortunately, the change in weight could not be determined as a small piece of the crystal broke off and was lost during the annealing process. The magnetic diffraction data are shown in fig. 6. The temperature dependence of the whole- and half-integral peak intensities behave qualitatively as observed for the x_2 sample. The plane ordering temperature returned to (essentially) the same value as for x_1 and x_2; $T_{Np} \approx 370$ K. The chain ordering temperature, on the other hand, increased to $T_{Nc} = 278(1)$ K, as indicated in fig. 6. Hence, it appears that the oxygen content is between that of the original as-grown crystal and $x_2 (\simeq 0.65)$.

We were able to measure the x_4 sample at temperatures up to 400 K, with the result that we explicitly observe $T_{Nc} \approx 370$ K as the temperature at which all magnetic Bragg intensities vanish. Fitting the $(\frac{1}{2}\frac{1}{2}2)$ intensity data for the temperature range $T \geq 290$ K to a Brillouin function gave an ordering temperature of 380 K, as shown in fig. 6, whereas a similar fit over the restricted temperature range 350 K $\geq T \geq$ 290 K increased the ordering temperature to 390 K. For the x_1 and x_2 data, T_N is therefore overestimated by 20 K from a mean field fit to the data. We have thus reduced the fitted values of the ordering temperatures for the x_1, x_2, and x_3 samples by 20 K in order to determine T_N. This is certainly a valid procedure for the x_2 sample, as the whole-integral intensity curves for x_2 and x_4 can be superimposed over the plane-only ordered region, indicating that T_{Np} is the same for both.

3. Results and discussion

At all four oxygen concentrations studied in this Pr1236+x sample, we have observed magnetic ordering of the Cu spins at approximately the same temperature of $T_{Np} \approx 370$ K. At the higher values of x, where only the Cu plane moments are ordered, we find that the spin structure is identical to that which has been previously observed for all the 123 plane-only ordering [8]: the Cu(2) spins are staggered along all three axes (see fig. 1(a)), and the moment directions are in the ab plane with a moment of $0.55(10)\mu_B$ at 300 K. We have found that the relative intensities of the whole-integral peaks agree fairly

well with the calculated intensities for this model, although there are some systematic discrepancies that are likely related to the magnetic form factor (eq. (2)). Detailed studies of the magnetic form factor will be the subject of a separate study.

The ordering of the Cu chains spins in this Pr1236+x single crystal is similar to the type of ordering that has been studied in detail in Nd1236.1 [8], but occurs at much higher temperatures (all greater than 150 K) than ever observed in "pure" 123 (all less than 100 K). Indeed, it is necessary to dope Nd onto the Ba site or Co to the Cu(1) site to get T_{Nc} so high. The effect of these substitutions implies that there is some electronic effect from these sites on the state of the chain Cu, and this is certainly consistent with the other observations for Pr1236+x, viz. the semiconducting behavior over the entire oxygen concentration range, the broad crystal-field levels, etc.

We have found, however, that there are some important differences between spin structures in the chain-ordered regimes for the Pr123 and Nd123 systems – in fact the relative intensities are quite different for the two materials. A detailed analysis for the Nd123 samples [8] showed that both the plane and chain moment directions are in the *ab* plane, with a chain moment that is about 40% of the plane moment at low temperature. If we fit the observed integrated intensities of Pr1236+x_2 at $T=20$ K to this Nd123 model (see fig. 1(b)), we obtain a Cu(1) moment of $0.2\mu_B$ and a Cu(2) moment of $0.85\mu_B$, at a relative angle of 15°. However, the fit to the data is not particularly good. A much improved fit to the observed intensities can be achieved if we relax the constraint on the Cu(1) moment so that it can have an ordered component along the *c*-axis, as indicated in fig. 1(c). We find that the *ab* plane components of Cu(1) and Cu(2) are 0.05 and $0.7\mu_B$, respectively, while the *c*-axis component of Cu(1) is $0.09\mu_B$. Thus we find that the chain moments are mainly along the *c*-axis.

The observation that T_{Nc} decreases substantially with increasing oxygen stoichiometry, while T_{Np} does not, reveals a very important difference between the Cu magnetism of Pr1236+x and the other $\mathscr{R}$1236+x compounds, which may be explained in light of recent optical reflectivity measurements on Pr1236+x [18]. For potentially superconducting $\mathscr{R}$1236+x compounds, on increasing the oxygen stoichiometry from $x=0$, the holes are initially doped mainly on the Cu(1) planes, and then mainly to the Cu(2) planes for $x>0.5$. The magnetic ordering of both the plane and chain Cu sublattices disappears near $x=0.5$. In Pr1236+x, Takenaka et al. [18] have observed that holes are not doped into the Cu(2) planes by the addition of oxygen, but are instead doped onto the Cu(1) sites and possibly the Pr ions. The intensitivity of the Cu(2) magnetism to the oxygen stoichiometry of Pr1236+x is consistent with the difficulty of doping holes onto the Cu(2) planes, whereas the decrease of T_{Nc} with increasing oxygen stoichiometry is consistent with the doping of holes onto the Cu(1) planes.

Acknowledgements

We thank B. Batlogg for the hyperbaric O_2 anneal, S. Skanthakumar and H. Zhang for their assistance with the single crystal X-ray measurements, and P.M. Grant for helpful conversations. Research at Maryland is supported by National Science Foundation Grant No. DMR 89-21878. Research within the National High Magnetic Field Laboratory is supported by National Science Foundation cooperative agreement DMR 90-16241.

References

[1] For a survey of the properties of $\mathscr{R}$1236+x compounds, see, e.g., High Temperature Superconductivity, ed. J.W. Lynn (Springer, Berlin, 1990).
[2] L. Soderholm, K. Zhang, D.G. Hinks, M.A. Beno, J.E. Jorgensen, C.U. Segre and I.K. Schuller, Nature (London) 328 (1987) 604.
[3] H.B. Radousky, J. Mater. Res. 7 (1992) 1917.
[4] W.-H. Li, J.W. Lynn, S. Skanthakumar, T.W. Clinton, A. Kebede, C.-S. Jee, J. E. Crow and T. Mihalisin, Phys. Rev. B 40 (1989) 5300.
[5] J.W. Lynn, J. Alloy Compunds 181 (1992) 419.
[6] S. Skanthakumar, W.-H. Li, J.W. Lynn, A. Kebede, J.E. Crow and T. Mihalisin, Physica B 163 (1990) 239.
[7] L. Soderholm, C.-K. Loong, G.L. Goodman and B.D. Dabrowski, Phys. Rev. B 43 (1991) 7923.
[8] W.-H. Li, J.W. Lynn and Z. Fisk, Phys. Rev. B 41 (1990) 4098.
[9] H. Kadowaki, M. Nishi, Y. Yamada, H. Takeya, H. Takei, S. Shapiro and G. Shirane, Phys. Rev. B 37 (1988) 7932.

[10] P.F. Miceli, J.M. Tarascon, L.H. Greene, P. Barboux, M. Giroud, D.A. Neumann, J.J. Rhyne, L.F. Schneemeyer and J.V. Waszczak, Phys. Rev. B 38 (1988) 9209.
[11] A.H. Moudden, G. Shirane, J.M. Tranquada, R.J. Birgeneau, Y. Endoh, K. Yamada, Y. Hidaka and T. Murakami, Phys. Rev. B 38 (1988) 8893.
[12] A. Keren, L.P. Le, G.M. Luke, B.J. Sternlieb, W.D. Wu, Y.J. Uemura, S. Tajima and S. Uchida, Bull. Amer. Phys. Soc. 37 (1992) 383.
[13] K.N.R. Taylor, P.S. Cook, T. Puzzer, D.N. Matthews, G.J. Russel and P. Goodman, J. Crystal Growth 88 (1988) 541.
[14] G.E. Bacon, Neutron Diffraction (Clarendon, Oxford, 1975).
[15] D.W. Cooke, R.S. Kwok, R.L. Lichti, T.R. Adams, C. Boekema, W.K. Dawson, A. Kebede, J. Schwegler, J.E. Crow and T. Mihalisin, Phys. Rev. B 41 (1990) 4801.
[16] T.M. Riseman, J.H. Brewer, E.J. Ansaldo, P.M. Grant, M.E. López-Morales and B.M. Sternlieb, Hyperfine Interactions 63 (1990) 249.
[17] M.E. López-Morales, D. Ríos-Jara, J. Tagüeña, R. Escudero, S. La Placa, A. Bezinge, V.Y. Lee, E.M. Engler and P.M. Grant, Phys. Rev. B 41 (1990) 6655.
[18] K. Takenaka, Y. Imanaka, K. Tamasaku, T. Ito and S. Uchida, Phys. Rev. B 46 (1992) 5833.